 DOI: 10.1002/masy.201000129

Diffusion Coefficients in Thermosensitive Poly(NIPAAm) Hydrogels

Aisha A. Naddaf, Hans-Jörg Bart*

Diffusion coefficients for the moving boundary thermosensitive poly(N-isopropylacrylamide) hydrogels, which were swelled to equilibrium in aqueous solutions of either BSA or phenol, have been determined. Using a uniaxial compression apparatus the collective (D_{col}) and with confocal Raman spectroscopy the mutual (D_{mut}) diffusion coefficients were estimated. The solute distribution in the hydrogel in addition to the effect of the swelling ratio, the cross-linking ratio and the hydrogel cylinder thickness on the Young's modulus were investigated.

Keywords: diffusion coefficient; mechanical properties; poly(NIPAAm) hydrogel

Introduction

Hydrogels, the water insoluble three dimensional polymeric networks, are known to have a high absorption capacity during swelling, which increase their initial volume several times without losing their original form. Due to their integrity and biocompatibility besides their degradability, hydrogels have wide applications in food additives pharmaceuticals and clinical applications fields. Moreover, hydrogels show an interested response to mechanical deformation but are still able to recover their initial shape. Hydrogels are also characterized by their stress-strain properties that ensure both; release of encapsulated materials in the delivery systems and strength in replacing cartilages. The mechanical properties are important for determining the utility of the polymer in an appropriate application.[1–3]

Poly(N-isopropylacrylamide) (poly(NIPAAm)) is a thermosensitive hydrogel and when heating it above its Lower Critical Solution Temperature (LCST), which is ranging between 32 °C–34 °C,[4] the internal structure changes from hydrated to a dehydrated state. It undergoes a reversible phase transition from a swollen (hydrated state) to a shrunken (dehydrated state), by which it loses about 90% of its mass.[5] Moreover, the LCST is close to the human body temperature and the gel has properties in common with soft biological materials like muscles and tendons.[6] Therefore, it has been investigated by many researchers for applications in biotechnological, medical, biological, and pharmaceutical fields (contact lenses, membranes for biosensors, sensors, actuators linings for artificial hearts and materials for artificial skin).[7–11] Such load bearing applications require an optimal hydrogel that is relatively strong and yet elastic. Controlling the polymerization conditions, such as temperature, light intensity, ionic strength and pH, play the main role in achieving the desired mechanical properties of the hydrogel.[12–13] Other techniques such as the addition of a compound[14] and thermal recycle[15] or changing the cross-linking density can also affect the hydrogel strength. The dependence of the mechanical desired properties of hydrogel on various parameters was summarized elsewhere.[9,16] It has been proposed as promising materials for biomedical implementations such as tendons, cartilages, replacing tissues damages, bones substitutes and in respect to advanced controlled drug delivery. Such applications of a biocompatible hydrogel, which is in direct contact with body fluids require

Chair of Separation Science and Technology, Kaiserslautern University, Gottlieb-Daimler Str. 44, 67653 Kaiserslautern, Germany
E-mail: bart@mv.uni-kl.de

ensuring both; accurate and targeted adsorption/desorption of an aqueous solution and a certain level of mechanical strength to keep its shape and performance.

In this work, the diffusion coefficient based in both Raman spectroscopy and the mechanical properties of the hydrogel were examined. For this purpose, different experimental setups were designed to measure the diffusion coefficient through a cylindrical hydrogel based on its viscoelastic properties as a function of its equilibrium temperature. Therefore, the determination of the collective diffusion coefficient, D_{col}, for the moving boundary thermosensitive poly(NIPAAm) hydrogels for aqueous phenol and BSA solutions was made in an uniaxial compression apparatus at different equilibrium temperatures of 25 °C, 32 °C, 37 °C and 40 °C. The collective diffusion coefficient was calculated using the correlation developed by Tanaka.[17] Besides, Raman spectroscopy was used as a modern non-destructive method to determine the mutual diffusion coefficient (D_{mut}) in thermo-sensitive poly-(NIPAAm) hydrogels for both solutions at 25 °C. The concentration dependency of the mutual diffusion coefficient (D_{mut}) was estimated at a fixed space location within the hydrogel cylinder over a long time period.

Experimental Part

Materials and Methods

The non-ionic N-isopropylacrylamide [NIPAAm, $H_2C{=}CHCONHCH(CH_3)_2$] (Aldrich > 97%) was polymerized without any further modifications from its monomer. The synthesis was achieved by free radical polymerization under oxygen-free conditions at 25 °C.[5,18,19] N,N-methylenbisacrylamide [MBA, $(CH_2{=}CHCONH)_2CH_2$] (Aldrich > 99.5%) was used as cross-linking monomer. Both sodium metabissulfite [NaDS, $Na_2O_5S_2$] (Aldrich > 98%) and ammonium-peroxodisulfat [APS, $(NH_4)_2S_2O_8$] (VWR, >98%) were used as initiators. Slightly yellow leaves of Bovine Serum Albumin protein [BSA] (Merck, >98%) were used to prepare the required BSA solutions which was used as drug example. Alternatively, aqueous phenolic solutions [C_6H_5OH] (MERCK, >98%) were used.

The synthesized hydrogel was characterized by calculating the hydrogel matrix ratio,[20] HMR given by:

$$HMR = \frac{m_{NIPAAm} + m_{MBA}}{\sum m_{tot}},$$
$$\text{where } m_{tot.} = m_{NIPAAm} + m_{MBA} + m_{H_2O} \quad (1)$$

Here m is the mass in [g], the subscripts NIPAAm, MBA, tot. and H_2O refers to N-isopropylacrylamide, N,N-methylenbisacrylamide, and water total mass respectively. The acceptable matrix ratio should be within the range of 0.08 - 0.12. The used poly(NIPAAm) in this work had a matrix ratio of 0.11. After the synthesis, the hydrogel was following several steps of cutting and washing before drying it over night at room temperature. Then, different samples of the dried hydrogel were immersed in different aqueous solutions of phenol (0.01 mM, 0.04 mM, 0.08 mM and 0.1 mM) and BSA (0.01 M, 0.05 M, 0.10 M and 1.51 M) and allowed to swell inside the air sealed containers to equilibrium by adsorbing the solution into the network for 48 hours at 25 °C.

Experimental Setup

Raman Spectroscopy

Figure 1 shows a description of the experimental setup used for measuring the mutual diffusion coefficient in hydrogel. The designed system consists mainly of Part 1, that contains the camera and the collective system, and Part 2, which includes the autofocus system and the diffusion cell. Raman spectra were recorded using a confocal spectrometer (Jobin-Yvon HR800) equipped with an internal exciting light source of HeNe ion laser polarized vertically with a power of 20 mW at a wavelength of 632.817 nm. After filtering out the plasma lines of the laser by using an appropriate interferential filter, the laser beam (H) is then

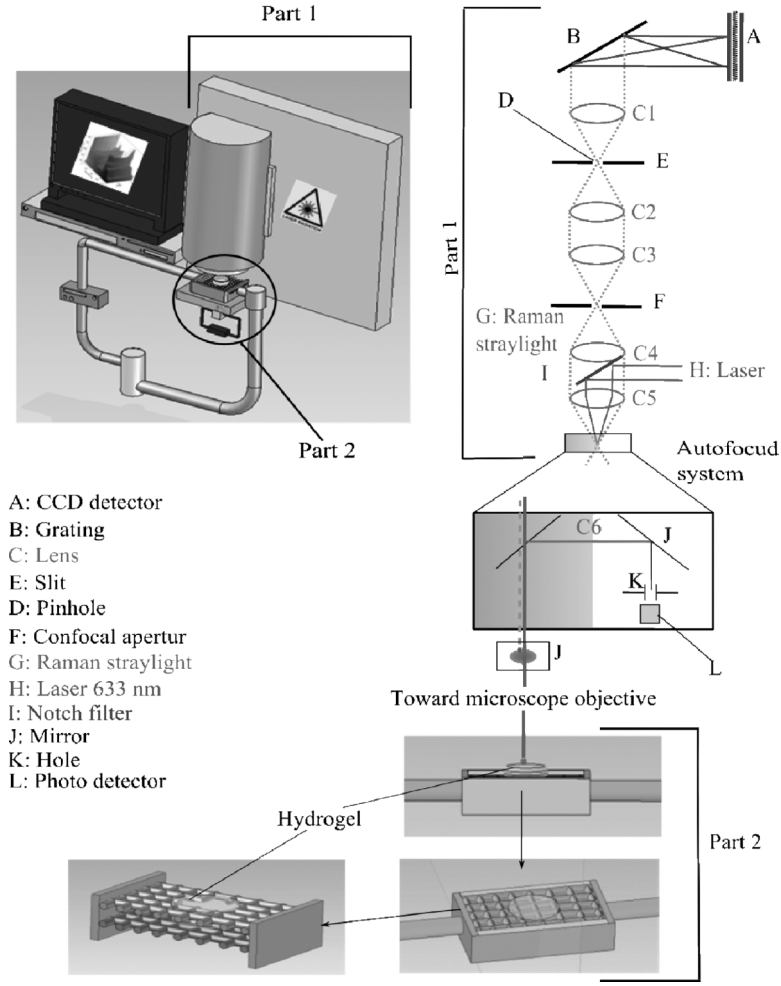

Figure 1.
Experimental setup to determine the mutual diffusion coefficient using Raman spectroscopy.[21]

completely reflected with an appropriate angle by the Laser Injection Rejection System (LIRS), which is composed of a mirror and the notch filter (I). The LIRS reflects the laser (H) towards the hydrogel sample through the diffusion cell (Part 2) under a microscope of high stability (BX 40) and focus graduation of 1 μm. Raman scattering is then totally collected and transmitted through a lens (C5), which produces a beam at an angle of 90° towards a confocal hole and the entrance slit of the spectrograph (K). The beam is coupled to a fiber optic and focused on the hydrogel sample using the 50xNA 0.7 microscope objective. A set of lens (C1-C3) focuses the signal toward the entrance slit (D) and the confocal aperture (F) of the spectrograph. The Raman signal is collected by the microscope objective in back scattering configuration follows the same way back. The reflection of the sample on the laser line (Rayleigh) is reflected again by the notch filter (I). Meanwhile, the passed Raman beam through the notch forms its image onto the entrance slit of the confocal hole (spectrograph) by the aid of lens 5 (C5). The spectrograph forms a spectrum on the photo detector (L) that has standard 1024X256 pixels of 26 microns. To detect

the spectra, a computer provided with Labspec software was connected to the CCD video camera (A) and Rio card for TV image digitalization. Raman spectroscopy measurements for all the hydrogel samples were carried out under the same optical conditions. A rectangular PVC diffusion cell with inner dimensions of $4.8 \times 1.3 \times 0.7$ mm was maintained at 25 °C and connected with a peristaltic pump (Samtec® REGLO FMI V1.05) to provide the solute loaded hydrogel cylinder with a continuous flow rate (1 ml/min) of deionized water (Figure 1- Part 2).

The transparent hydrogel cylinder, which is located in the diffusion cell and immersed in the flowing solution, is assumed to absorb a negligible amount of energy. The diffusion cell was designed in a way to keep the hydrogel samples fixed in position by being sealed with a metal grid to prevent sample movement caused by the flow of water. Moreover, to avoid the evaporation of the solution due to the exposing to the ambient air, the hydrogel sample box was covered with microscope slide including a central tiny hole that allow the laser to transmit directly to the hydrogel at the required detecting point.[21]

Mechanical Properties

The mechanical properties examination in addition to the collective diffusion coefficient measurements were accomplished at a thermostated environment of 25 °C using an uniaxial compression apparatus (see Figure 2). A vertical load was applied manually on the cylindrical hydrogel samples, with various degree of swelling, and were placed directly above a digital libra (L610-**D Sartorius GmbH). The transmitted compression force (and the applied stress) to the hydrogel cylinder was calculated from the reading of the balance. Meanwhile, the resulting deformations (associated strain) were detected using a microscope (Stemi SV 11) connected to a colour video camera (JVC.TK-C1381) and an objective (Imtronic GmbH). The required measurements were carried out accurately using a PC provided with a Grab&View® software and Image-C program®.

Results and Discussion

Characterization and Image Analysis

Raman spectroscopy has been considered as an effective method to characterize the chemical structure of hydrogels.[5] Figure 3 shows Raman spectrum of poly(NIPAAm) hydrogel immersed to equilibrium in a phenol solution of 0.10 mM. Raman spectrum of water is found due to the O-H stretching vibration to be an abroad band between 3200 and 3735 cm^{-1} and the distinct peak for the isopropyl group at 2925 cm^{-1} is a characteristic signal of

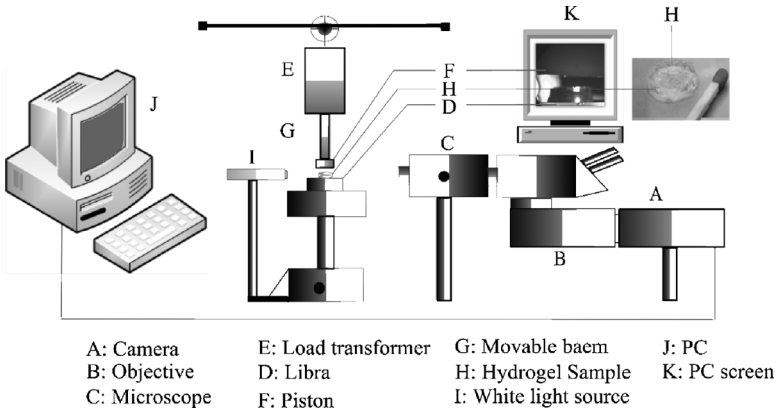

Figure 2.
The uniaxial compression system.

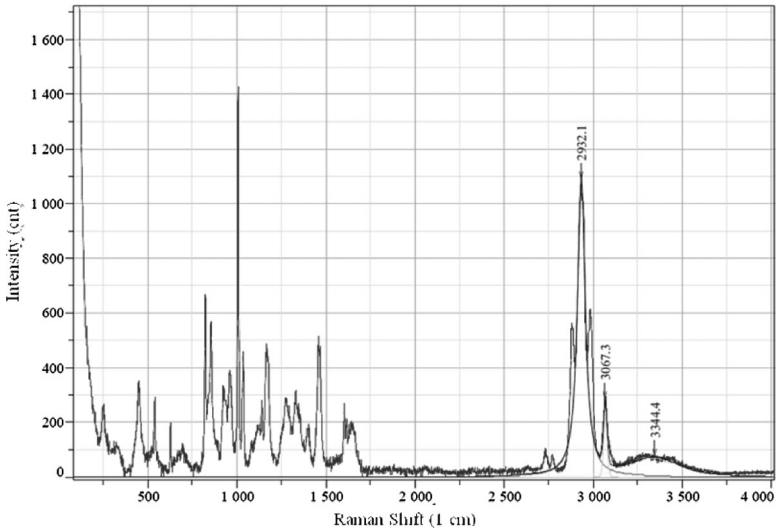

Figure 3.
Expanded Raman spectrum for the poly(NIPAAm)/phenol system.[21]

poly(NIPAAm).[22–23] Next to it particularly at 3066 cm^{-1}, another small distinct peak was observed to refer of the presence of phenol.[5,21] Such a characteristic peak was not possible to be distinguished for BSA, since the Raman spectra of BSA resulted from the CH_3-stretching vibration, which integrates from 2910 to 2965 cm^{-1}, is also caused from the poly(NIPAAm) signal.[24] The Raman spectra were obtained at fixed spatial position within the hydrogel near the outer surface for both solutes. A transient Raman intensity map for the poly(NIPAAm)/BSA system is given in Figure 4. The variation of the distinct peak intensity at 2925 cm^{-1} shown in Figure 4 relates to the change in the concentration of the BSA inside the poly-(NIPAAm) hydrogel during the diffusion. The regulated time interval between two

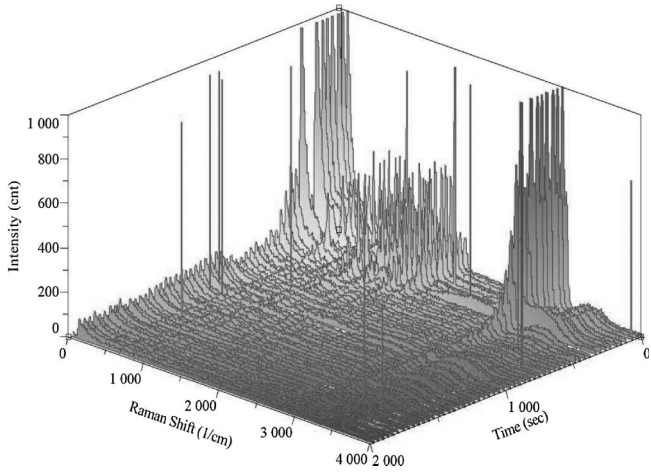

Figure 4.
Transient Raman map for the poly(NIPAAm)/BSA system at a fixed spatial position.

spectrums was 10 sec. At the beginning of the diffusion, the spectra have a high peak signal and refer to the high concentration of BSA in hydrogel. With time, the height of the peaks (and the concentration of the BSA in the hydrogel) starts to decrease gradually compared to the water band till it become constant.

The deionized water starts to diffuse into the gel initially at time $t = 0$ by remaining the concentration at the hydrogel/solution interface poly(NIPAAm) C_o constant. The minimal amount of solute dissolving into the flowing cell reservoir during the experiment is negligible. The diffusion coefficient (D) was calculated as a function of concentration (C) at distance x from the interface at elapsed time interval t by assuming a semi-infinite media[25,26] according to the equation:

$$C = C_o \cdot erf\left[x \Big/ 2\left(\sqrt{D \cdot t}\right)\right] \quad (2)$$

By assuming the hydrogel as a semi-infinite media, the diffusion of the solute out of the hydrogel can be studied and analyzed via Raman spectroscopy by replacing the concentration term in the developed expression of equation (2) with the intensity.[21] To determine the relation between the initial solute concentration and Raman intensity, different samples of poly(NIPAAm) cylinders were allow to swell at 25 °C to equilibrium in BSA and phenol solutions at different concentrations. From this, two calibration curves (for BSA and phenol) resulted relating the Raman intensity ($I_{CH}(t,x)$) to the solute concentration as follows:[21]

$$I_{CH,H_2O}of\left(C_{solution(phenol,BSA)}(t,x)\right) = I_{CH}^{\text{int}} \cdot erf\left[x \Big/ 2\left(\sqrt{D_{mut} \cdot t}\right)\right] \quad (3)$$

I_{CH}^{Int} is the intensity at the hydrogel/water interface boundary and D_{mut} is the mutual diffusion coefficient. For each data point in Figure 4, the mutual diffusion coefficient was calculated from equation (3) using Matlab® and then the average diffusion coefficient had been determined.

Viscoelastic Characterization

Mechanical Behavior

With the designed compression test apparatus, the applied load was increasing gradually on the individual poly(NIPAAm) cylinders in their swollen state by a force step of 0.2N. Depending on the equilibrium conditions, some poly(NIPAAm) cylinders were able to bear a force up to 4N without breaking down. The initial diameter of the hydrogel cylinder affects the final force the hydrogel can withstand. Figure 5 and 6

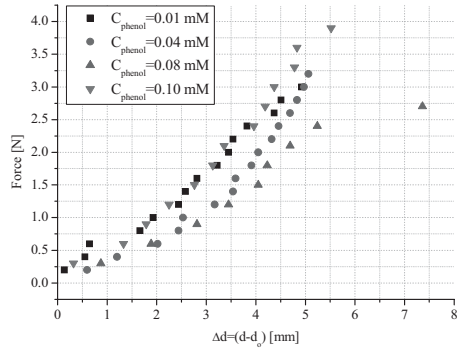

Figure 5.
Force versus diameter change of four poly(NIPAAm) cylinders of different initial diameters ($d_o =$ ■ 13.156 mm; ● 13.064 mm; ▲ 12.42 mm; ▼ 13.064 mm) and different concentrations of phenol at 25 °C.

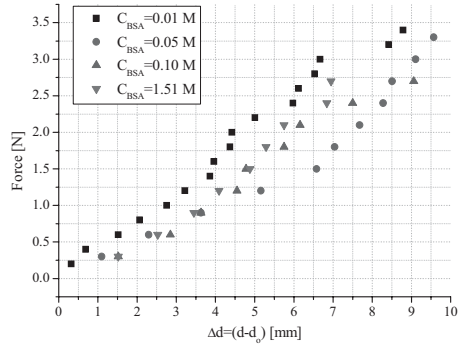

Figure 6.
Force versus diameter change of four poly(NIPAAm) cylinders of different initial diameters ($d_o =$ ■ 12.742 mm; ● 13.478 mm; ▲ 11.914 mm; ▼ 12.006 mm) and different concentrations of BSA at 25 °C.

show force versus diameter change of poly(NIPAAm) cylinders of different initial diameters, d_0 and different concentrations of phenol and BSA at 25 °C respectively. The measuring time of the data points, which were ranging according to the hydrogel cylinder conditions between 9 and 17 points, was kept as short as possible to avoid weight loss due to evaporation in the open system. The resulted relation between the applied load and the deformations seems to be non-linear and poly(NIPAAm) cylinders with a high initial diameter can withstand higher load.

Meanwhile, a larger force is required to obtain a given degree of deformation for the thicker poly(NIPAAm) cylinders as can be seen from Figure 7 and 8. The minus sign of the thickness change, Δl refers to the reduction of thickness due to the uniaxial applied load.

Typical obtained stress-strain data are shown in Figure 9. The included insets show the images of the hydrogel cylinder at the corresponding deformation. The shown poly(NIPAAm) hydrogel cylinder consists of a MBA mole fraction of 0.0115 and exhibits a sigmoidal stress-strain relationship in the elastic region, which ended at 7 MPa. The stress continues rising until the hydrogel cylinder ruptures. This typical curve is affected by change of temperature and concentration.

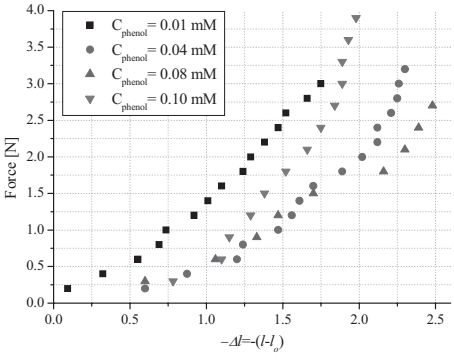

Figure 7.
Force versus thickness change of four poly(NIPAAm) cylinders of different initial thicknesses (l_o = ■ 2.852 mm; ● 3.772 mm; ▲ 3.588 mm; ▼ 2.944 mm) and different concentrations of phenol at 25 °C.

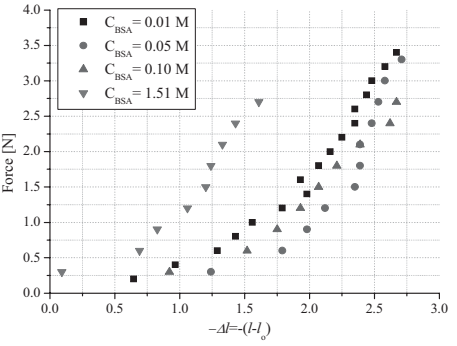

Figure 8.
Force versus thickness change of four poly(NIPAAm) cylinders of different initial thicknesses (l_o = ■ 3.634 mm; ● 3.358 mm ; ▲ 3.818 mm; ▼ 3.22 mm) and different concentrations of BSA at 25 °C.

As can be seen from Figure 10 and 11 both hydrogel/phenol and hydrogel/BSA loaden cylinders show a lower linear strain response below the LCST, which indicates the demonstration of the elastic behavior. For example, at 25 °C the maximum strain was not exceeding 75% for phenol and BSA with a corresponding maximal compression stress of 0.0144 MPa and 0.009 MPa respectively. Similarly, at 32 °C the maximum achieved strain was 83% for phenol and 79% for BSA. At higher temperatures, the linear strain response, which is combined with a dynamic viscoelastic behavior, becomes more remarkable till reaching its maxima. The hydrogel/phenol cylinder was able to reach 90% deformation at 40 °C and withstand a maximum stress of 0.195 MPa without rupture (Figure 10). Less maximum deformation of 85% was achieved for the hydrogel/BSA cylinder. Here the concentration of the solute plays a minor role in the hydrogel lattice deformation.

As can be seen from Figure 10 and 11, each sample was subsequently deformed to a specific compressive strain level, by which the strain changes proportionally with the applied load. Moreover, the stress increases strongly from 25 °C to 40 °C. This behavior may be better understood by relating it to the dependency of the swelling ratio on the temperature presented in Figure 12. By increasing the temperature, the hydrogel

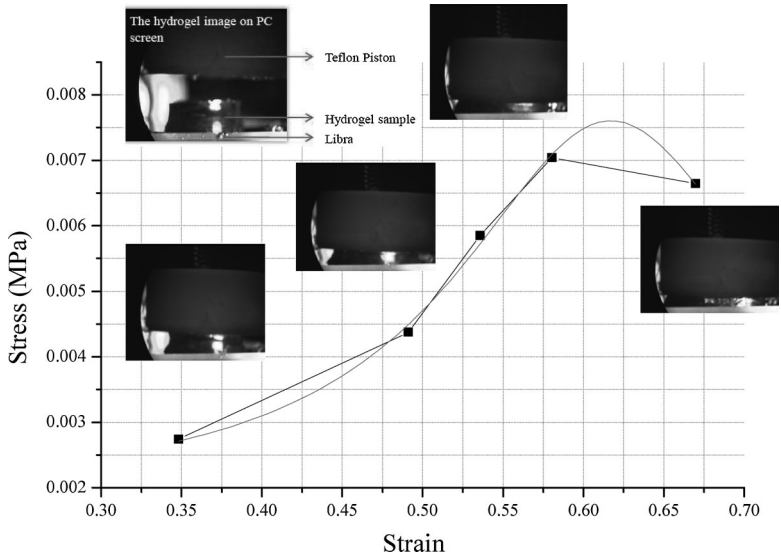

Figure 9.
Stress-strain data for poly(NIPAAm) of a matrix ration of 0.105 after swelled to equilibrium at 25 °C in deionized water.

shrinks and becomes harder due to the denser network. By temperature elevation from 25 °C to 37 °C for hydrogel/phenol system, the compressive stress increased from 0.015 MPa up to 0.20 MPa. For the same temperature elevation range, the compressive stress increased from about 0.008 MPa up to 0.12 MPa for the hydrogel/BSA system. The increase in the compressive stress of hydrogel/phenol cylinder can be related to the contribution of phenol molecules, which participate in forming a dense layer of the hydrogel network.[27,28] In both cases, the increase of the compressive stress may suggest that the temperature elevation influences the mechanical properties and leads to a stronger, hydrogel.

Compression Failure

The Young's Modulus (Y) for the hydrogels of different swelling ratios was determined from the initial portion of the stress-strain data in compression test using the equation:

$$Y \equiv \frac{Stress}{Strain} = \frac{F/A_\circ}{\Delta l/l_\circ} = \frac{Fl_\circ}{A_\circ \Delta l} \quad (4)$$

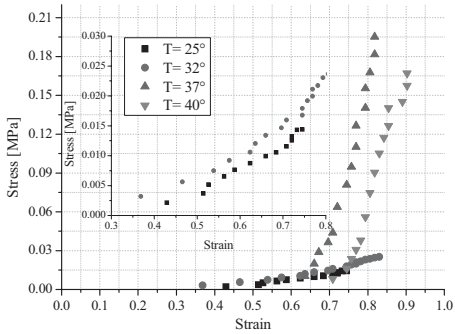

Figure 10.
Stress-strain curves for hydrogels swelled in 0.10 mM phenol solution at different temperatures.

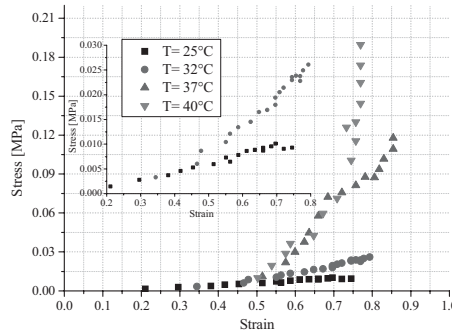

Figure 11.
Stress-strain curves for hydrogels swelled in 0.01 M BSA solution at different temperatures.

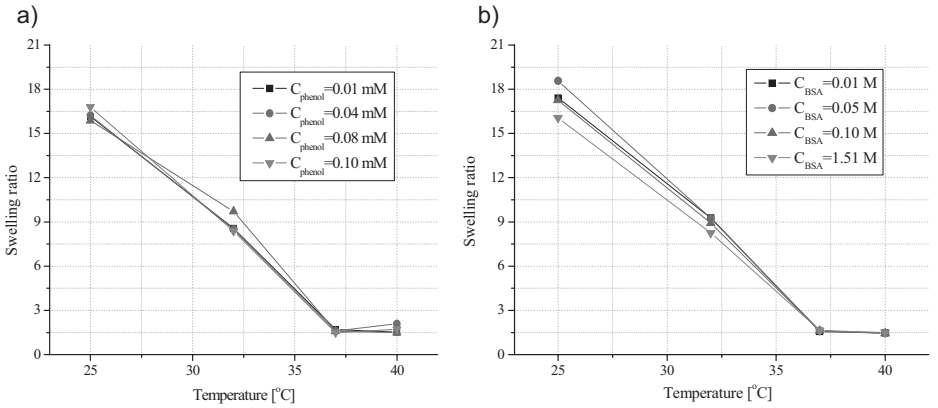

Figure 12.
Swelling ratio as a function of temperature for poly(NIPAAm) immersed to equilibrium in (a) phenol and (b) BAS.

F is the uniaxial force acting per unit cross-sectional area (A_o), Δl is the deformation ratio and l_o is the initial thickness. The behavior of a hydrogel submitted to a continuous stress increase was monitored until the maximum deformation was reached. Figure 13 shows the Young's Modulus change by varying the swelling ratio of hydrogel cylinders swelled to equilibrium in different concentrations of phenol solutions. The same is with BSA in Figure 14.

As presented in Figure 13 and 14 , the rapid changes of the Young modulus at a certain swelling ratio degree are clearly contributed due to the temperature elevation and are less sensitive to concentration changes. Exceeding the LCST expels the liquid from the hydrogel lattice causing substantial increase in the Young modulus from about 0.14 MPa for 0.1 mM phenol solution and about 0.3 MPa for 1.51 M BSA compared to 0.02 MPa for 0.1 mM phenol solution and about 0.035 MPa for 1.51 M BSA at 25 °C. At this rage of temperatures, the poly(NIPAAm) forms a physical entanglements, which increases the apparent cross-linking density of the hydrogel and then the compressive elastic modulus.[2,29] The effect of the concentration of solute (phenol or BSA) shows less effect on the Young modulus compared to the effect of

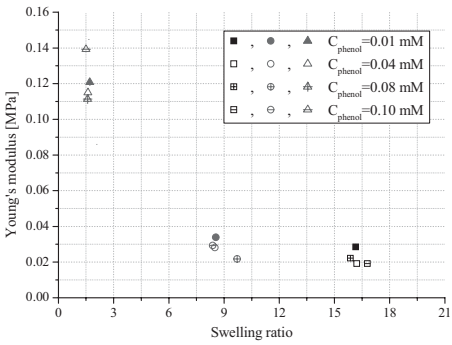

Figure 13.
Young's modulus variation for different phenol solutions at different temperatures: (■) 25 °C; (●) 32 °C; (▲) 37 °C.

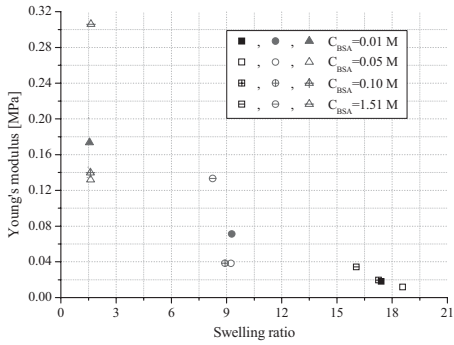

Figure 14.
Young's modulus variation for different BSA solutions at different temperatures: (■) 25 °C; (●) 32 °C; (▲) 37 °C.

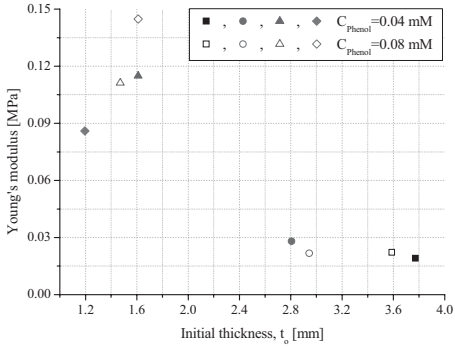

Figure 15.
Young's modulus for hydrogels swelled in 0.04 mM and 0.04 mM phenol solution at different temperatures: (■) 25 °C; (●) 32 °C; (▲) 37 °C; (◆) 40 °C.

temperature. Nevertheless, the deviation in the Young modulus with changing BSA concentration is more obvious than that of phenol.

The calculated Young's modulus variation with initial thickness is illustrated in Figure 15 and 16 for phenol and BSA respectively. The cross sectional areas combined with hydrogel cylinder deformation were measured with the aid of the optical microscope and the image analysis software described above. The obtained results indicate that the mechanical strength of the hydrogel cylinders is decreasing with increasing the thickness of the sample.

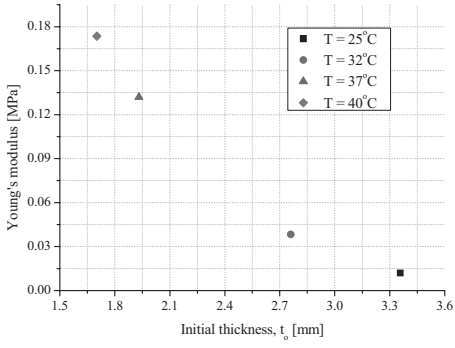

Figure 16.
Young's modulus for hydrogels swelled in 0.05 M BSA solution at different temperatures.

Based on the experimental values obtained from the compression measurements (Table 1), the viscoelastic properties were calculated using Matlab®. Then, the numerical values were used to calculate the collective diffusion coefficient, D_{col} using the Tanaka-Fillmore equation:[17]

$$D_{col} = \left(K + \frac{4\mu}{3}\right) \Big/ f \tag{5}$$

$$K = Y/3(1-2v) \tag{6}$$

$$\mu = Y/2(1+v) \tag{7}$$

Here K is the bulk modulus [N/m^2], μ is the shear modulus [N/m^2], v is the Poisson's ratio and f is the friction coefficient, which describes the viscous interaction between the polymer and the solvent. As mentioned previously, the Young's Modulus was determined from the initial part of the stress-strain data of the compression test using equation (4).

Diffusion Coefficient

Mutual Diffusion Coefficient

To determine the mutual diffusion coefficient as a function of the solute concentration, several samples were loaded to equilibrium in phenol solutions as mentioned above. By using equation (3), the variation of the average calculated mutual diffusion coefficient at 25 °C was determined (see Figure 17). As the concentration of phenol increases the mutual diffusion coefficient also increases. Similar results, indicating that the diffusion coefficient is concentration-dependent, have been reported in the literature.[30,31] This dependency of diffusivity on concentration was found to be as a result of the solute-hydrogel interaction.[32] For the varied concentrations of loaded phenol; 0.01 mM, 0.04 mM, 0.08 mM and 0.1 mM, the corresponding average diffusion coefficients were 5.6185×10^{-11}, 1.64338×10^{-10}, 2.87919×10^{-10} and 3.34565×10^{-9} m^2/s respectively, as reported in previous work.[21] Although the change of the concentrations studied here is significant,

Table 1.
Experimental data obtained from the compression measurements and used to calculate the collective diffusion coefficient.

Material	Concentration (M)	T(°C)	Diameter, *d* (m)		Thickness, *l* (m)		Diffusion coefficient, $(m^2/s) \times 10^{-9}$
			Initial	Final	Initial	Final	
Phenol	10^{-5} M	25	0.013156	0.015088	0.002852	0.002116	0.0074
Phenol	10^{-5} M	37	0.005336	0.005704	0.001242	0.000782	0.0855
Phenol	10^{-5} M	40	0.004622	0.004830	0.001932	0.001518	0.1939
Phenol	$4 \cdot 10^{-5}$ M	25	0.013064	0.015594	0.003772	0.002300	0.0056
Phenol	$4 \cdot 10^{-5}$ M	32	0.010120	0.012420	0.002806	0.001564	0.0070
Phenol	$4 \cdot 10^{-5}$ M	37	0.004922	0.005290	0.001610	0.000874	0.0840
Phenol	$4 \cdot 10^{-5}$ M	40	0.005244	0.005934	0.001196	0.000552	0.0518
Phenol	$8 \cdot 10^{-5}$ M	25	0.012420	0.015226	0.003588	0.002254	0.0035
Phenol	$8 \cdot 10^{-5}$ M	32	0.010212	0.012466	0.002944	0.001288	0.0082
Phenol	$8 \cdot 10^{-5}$ M	37	0.004784	0.005474	0.001472	0.000736	0.0607
Phenol	$8 \cdot 10^{-5}$ M	40	0.005290	0.005566	0.001610	0.001104	0.1074
Phenol	10^{-4} M	25	0.013064	0.014858	0.002944	0.001794	0.0092
Phenol	10^{-4} M	32	0.009752	0.012374	0.003220	0.001748	0.0041
Phenol	10^{-4} M	37	0.004876	0.005382	0.001794	0.001104	0.0826
Phenol	10^{-4} M	40	0.005474	0.005792	0.001288	0.000828	0.0883
BSA	10^{-2} M	25	0.012742	0.015502	0.003634	0.002070	0.0049
BSA	10^{-2} M	32	0.010166	0.011500	0.002392	0.001978	0.0070
BSA	10^{-2} M	37	0.004692	0.005336	0.002070	0.001380	0.0731
BSA	10^{-2} M	40	0.005060	0.005474	0.002024	0.001334	0.0934
BSA	$5 \cdot 10^{-2}$ M	25	0.013478	0.017112	0.003358	0.001380	0.0032
BSA	$5 \cdot 10^{-2}$ M	32	0.009982	0.012466	0.002760	0.001840	0.0002
BSA	$5 \cdot 10^{-2}$ M	37	0.005198	0.005888	0.001932	0.001242	0.0614
BSA	$5 \cdot 10^{-2}$ M	40	0.004968	0.005382	0.001702	0.001196	0.1033
BSA	10^{-1} M	25	0.011914	0.015548	0.003818	0.002070	0.0006
BSA	10^{-1} M	32	0.010074	0.012190	0.002116	0.001426	0.0052
BSA	10^{-1} M	37	0.005060	0.005888	0.002070	0.001334	0.0494
BSA	10^{-1} M	40	0.005106	0.005382	0.002024	0.001288	0.1022
BSA	1.51 M	37	0.004876	0.005474	0.001840	0.001518	0.0479
BSA	1.51 M	40	0.004876	0.005336	0.002070	0.001518	0.1026

the values obtained for the mutual diffusion coefficient of poly(NIPAAM)/BSA only varied slightly; from $5.67 \cdot 10^{-14}\,m^2/s$ to $6.07 \cdot 10^{-14}\,m^2/s$ for 1.51 M to 0.1M respectively. Nevertheless, these values are still closed to reported effective diffusion coefficient of acrylamide hydrogel/BSA system,[34] which indicates an increasing resistance to diffusion inside the hydrogel due to a high swelling ratio. In another case study it was found, that the mutual diffusion coefficient is strongly influenced by the internal gel properties, as is the average free hole volume.[33] Hence larger average free hole volume will lead to larger diffusivity at a given solute concentration. For a solute with a high molecular weight (such as BSA), the network has a considerable effect on diffusion i.e. the diffusivity in a thermosensitive hydrogel is restricted by obstruction phenomenon for large molecules.[34] However, this as a result gives diffusion coefficients for BSA at about 4 magnitudes smaller as phenol.

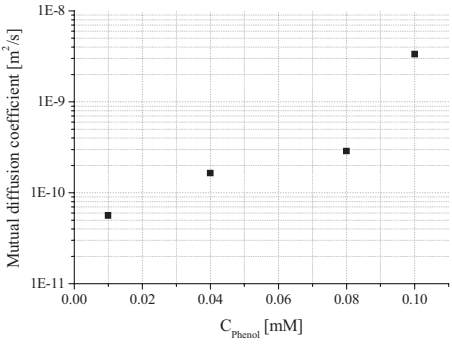

Figure 17.
Averaged mutual diffusion coefficients for different initial phenol concentrations.

Collective Diffusion Coefficient

As can be seen from Figure 18, regardless to the used phenol concentration, the diffusion coefficient is identical at 25 °C and 32 °C (below and around the LCST). Meanwhile, above the LCST the diffusion coefficient varied significantly. Nevertheless, the temperature elevation, which is playing a remarkable role in shrinking the hydrogel, causes an increase in the diffusion coefficient in the hydrogel/phenol system (see Figure 18). For the hydrogel/BSA system, the diffusion coefficient increased also with increasing temperature, but with less divergence above the LCST compared to hydrogel/phenol system. The concentration of BSA has less effect on shrinking compared to the interactions caused by the ring-shaped phenol molecule, which can act as a proton donor or acceptor.[27] More about the effect of phenol on the thermosensitive hydrogel is available elsewhere.[28]

At 25 °*C*, the diffusion coefficient of the hydrogel cylinder immersed to equilibrium in the 0.01 mM phenol equals 7.4×10^{-12} m/s^2 and this value increased about two orders of magnitude by increasing temperature to reach $1.939 \times 10^{-10}\,m/s^2$ at 40 °C. The effect of temperature on the diffusion coefficient is following the same trend for all phenol concentrations. Nevertheless, at the highest concentration of phenol, which also maximal effects the hydrogel shrinking at low temperatures, is responsible for decreasing the diffusion coefficient compared to the lowest concentration of 0.10 mM phenol in an order of magnitude, as is from $9.2 \times 10^{-12}\,m/s^2$ to $8.83 \times 10^{-11}\,m/s^2$.

The diffusion coefficient of 0.01M BSA was varying from $4.9 \times 10^{-12}\,m/s^2$ at 25 °C to reach $9.34 \times 10^{-11}\,m/s^2$ at 40 °C (see Figure 19). The effect of temperature on the diffusion coefficient is following the same trend for all BSA concentrations. In contrast to phenol, the higher concentration of BSA has almost no remarkable effect on changes of the diffusion coefficient, i.e. it increased for the 1.5M BSA from $1.29 \times 10^{-11}\,m/s^2$ to $1.026 \times 10^{-10}\,m/s^2$. This related to the mechanical strength measurements of the hydrogel swelled in BSA protein, which demonstrated that the Young's modulus does not vary with the presence of proteins.[36] The direct effect of the Young's modulus on the collective diffusion coefficient appears in equation (5) and (6). Compared to the collective diffusion coefficient, a higher measured mutual diffusion coefficient was obtained for different concentrations of phenol at 25 °C (Figure 20). This diversity in the values of diffusion coefficient between both methods is mainly related to the effect of hydrogel cylinder dimensions. The collective diffusion coefficient determination was based on the work of Tanaka,[17,37] which relates the swelling of the gel to the gradient of the stress and

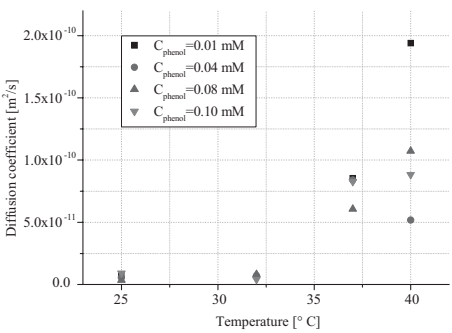

Figure 18.
D_{col} with temperature change for different concentrations of phenol.

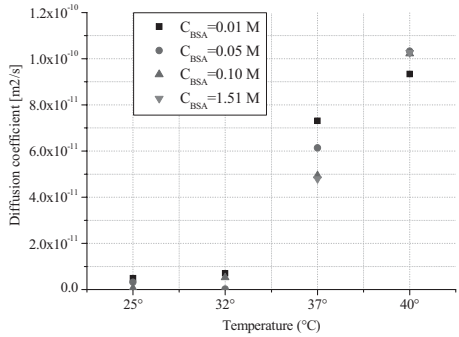

Figure 19.
D_{col} with temperature change for different concentrations of BSA.

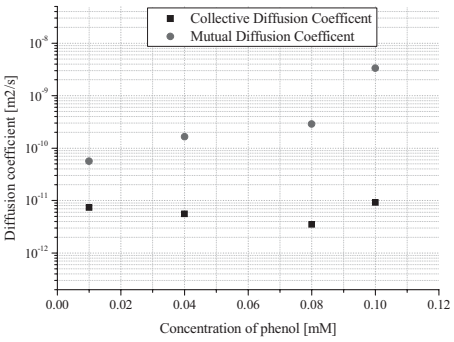

Figure 20.
Comparison between the D_{col} and D_{mut} for different concentrations of phenol at 25 °C.

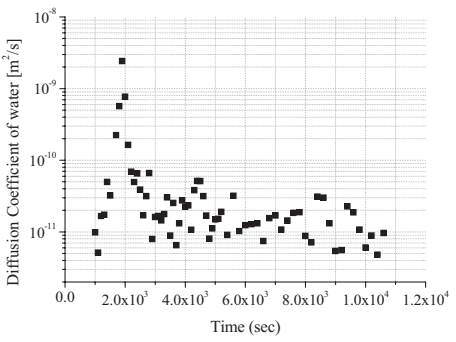

Figure 21.
The effect of the scattered intensity on the mutual diffusion coefficient as a function of time for phenol (0.01 mM) at 25 °C.

describes small volume changes during swelling i.e. the diffusion coefficient is dependent on the hydrogel geometry.[38,39] The effect of the geometry and dimensions of the hydrogel on the obtained collective diffusion coefficient was found to be dependent on the shear modulus, which reduces the speed of diffusion in the diffusion direction. In other words, for a cylinder, the diffusion occurs in two dimensions (radial and axial) and it is combined with volume change. Due to the existence of the shear modules, the shear relaxation process occurs and causes a volume change in the diffusion directions. This geometrical constraint results in a reduction of the speed of the diffusion in the diffusion directions.[40,41] In contrast to this, the effect of the dimensions of the hydrogel cylinder is playing no role in the case of measuring the mutual diffusion coefficient using Raman Spectroscopy. Moreover, the mutual diffusion coefficients of BSA and phenol were obtained based on Raman Spectra, which can be recorded without any major interference from geometrical changes or from the water band.[26]

In addition, although the hydrogels were taken from the same synthesized batch and have the same geometries, the effect of the local dynamic inhomogeneity appears. The dynamic inhomogeneity is found to be as a result of the difference in the molecular environment, e.g., the difference in the local gel concentration and/or cross-linking density. It may also occurs due to the distributions of the holes in the lattice and the as a result of the swelling of hydrogel happing during the diffusion. This inhomogeneity may affect the scattered intensity[42] and as consequence gives different local data in the long term averaged measurement based on Raman spectroscopy (Figure 21) to calculate the mutual diffusion coefficient.

Conclusion

For the thermosensitive poly(N-isopropylacrylamide) hydrogels (poly(NIPAAm)), which were swelled to equilibrium in different concentrated phenol and BSA solutions, the collective diffusion coefficient was calculated after a model from literature, which bases on measurement of the bulk modulus, the shear modulus and the frictional coefficient between the solvent and the hydrogel network. Additionally, the relation between the solvent concentration and Raman intensity of the poly(NIPAAm)/solvent system, which is changing during the continuous diffusion of the solvent through the hydrogel was employed to calculate the mutual diffusion coefficient.

Poly(NIPAAm) hydrogels was load and allowed to swell to equilibrium with either aqueous phenol or BSA solutions. The phenol solutions prepared were 0.01 mM,

0.04 mM, 0.08 mM and 0.1 mM and the BSA solutions were 0.01 M, 0.05 M, 0.10 M and 1.51 M. An uniaxial compression apparatus was designed to examine the mechanical properties and to determine the collective diffusion coefficient in poly(NIPAAm) hydrogels equilibrated in different solute concentrations at 25 °C, 32 °C, 37 °C and 40 °C. Depending on the equilibrium conditions, the poly(NIPAAm) cylinders were able to bear an axial load up to 4 N without break down. The lower initial diameter is a main factor that effects the final force that the hydrogel can withstand i.e., the poly-(NIPAAm) cylinder with a lower initial diameter can withstand a higher load. However, a larger force is required to obtain a given degree of deformation for the thicker poly(NIPAAm) cylinders. Poly(NIPAAm) hydrogel cylinders exhibit a sigmoidal stress-strain relationship in the elastic region. This typical curve is affected by temperature and the composition of the equilibrium solution in the linear stress domain until rupture. At higher temperature, the hydrogels need a higher stress for a given deformation and remain in the elastic state even by reaching 90% of the maximal applied strain. Moreover, the stress increases strongly from 25 °C to 40 °C. This behavior may be better understood relating it to the dependency of the swelling ratio on the temperature which increases the hardness of the hydrogel due to the shrinking. Therefore, the temperature elevation is suggested to influence the mechanical properties and leads to a mechanical stronger hydrogel. Both hydrogel/phenol and hydrogel/BSA cylinders show a linear strain response combined with a dynamic viscoelastic behavior below the LCST. At higher temperatures, this becomes more remarkable till reaching its maximal stress. The Young modulus is affected at a certain swelling ratio degree with the temperature elevation.[2,30] The hydrogel cylinders subjected to a load at high temperatures (i.e. 37 °C) have less elasticity. The concentration of phenol and BSA shows less effect on the Young modulus compared to the effect of temperature. Nevertheless, less maximal deformation of 85% was achieved for the hydrogel/BSA cylinder in which the concentration of the diffusing solute plays a minor role in the deformation of the hydrogel lattice. In compression test, the Young modulus was determined from the initial portion of the stress-strain data. The obtained results indicate that the mechanical strength of the hydrogel cylinders is decreasing with increasing the thickness of the sample.

From the compression measurements and by using a Matlab® Program, the viscoelastic properties such as the Young's modulus, the shear modulus and the bulk modulus were calculated and used to calculate the collective diffusion coefficient based on the Tanaka-Fillmore equation.[17] The diffusion coefficients below and around the LCST are almost identical. Meanwhile, above the LCST the diffusion coefficient varied significantly. The temperature elevation from 25 °C to 40 °C caused an increase in the diffusion coefficient of hydrogel/0.01 mM phenol system within two orders of magnitude. The higher concentration of phenol affects the hydrogel shrinking, even at low temperatures, and increases the diffusion coefficient of the hydrogel/0.1 mM phenol system with only one order of magnitude at temperature elevation from 25 °C to 40 °C. Similarly, the diffusion coefficient of the hydrogel/BSA system increases by increasing the temperature but with less divergence above the LCST compared to hydrogel/phenol system since the concentration of BSA has less effect in shrinking compared to ring-shape phenol molecule.

Besides obtaining information about the chemical composition of the hydrogel/phenol system, Raman spectroscopy was used to study the change of intensity with the solute concentration during the diffusion, from which the mutual diffusion coefficient in the thermosensitive poly(NIPAAm) hydrogel loaded with different initial concentrations of phenol (0.01 mM, 0.04 mM, 0.08 mM and 0.1 mM) at a selected temperature of 25 °C was measured. It was found that the diffusion

coefficient increases by increasing the concentration of phenol.[30,31] The mutual diffusion coefficient varied from 5.61845×10^{-11} to $3.34565 \times 10^{-9}\,m^2/s$ for the hydrogel cylinder loaded with phenol concentration of 0.01 mM and 0.1 mM respectively. This dependency of diffusivity on concentration is due to the solute-hydrogel interaction.[32] Although the change of the concentrations studied here is significant, the values obtained for the mutual diffusion coefficient of poly(NIPAAM)/BSA only varied slightly; from $5.67 \cdot 10^{-14}\,m^2/s$ to $6.07 \cdot 10^{-14}\,m^2/s$ for 1.51 M to 0.1M respectively. The results, compared to phenol, indicates an increasing in resistance to diffusion inside the hydrogel due to a high swelling ratio and/or the average free hole volume, which strongly influences the mutual diffusion coefficient.[33] The larger average free hole volume of a solute with a high molecular weight (such as BSA) leads to larger diffusivity at a given solute concentration.[34]

Although the hydrogels were taken from the same synthesized batch, the comparison between the collective and mutual diffusion coefficients shows a higher measured mutual diffusion coefficient for different concentrations of phenol at 25 °C. This diversity in the values of diffusion coefficient between both methods is related to different effects. The dimensions of the hydrogel cylinder affect directly the collective diffusion coefficient, which its determination based on relating the swelling of the gel to the gradient of the stress and the value of the diffusion coefficient using this method is affected even with small volume changes during swelling.[38,39] Moreover and due to the existence of the shear modules, the shear relaxation process occurs and causes a volume change that influence the value of the collective diffusion coefficients.[40,41] However, the effect of the dimensions of the hydrogel cylinder is playing no role in the case of measuring the mutual diffusion coefficient using Raman spectroscopy. Nevertheless, the local dynamic inhomogeneity may cause the scattered intensity and as consequence gives different local data in the long term to calculate the mutual diffusion coefficient.[42] In principle, Raman spectroscopy is a powerful technique for the investigation of the diffusion phenomena through poly-(NIPAAm)/phenol as a function of time and distance from the hydrogel surface.

Acknowledgements: The authors wish to acknowledge the German Research Foundation (DFG) and the State Research Unit "Advanced Materials Engineering" (AME) for the financial support.

[1] A. Hakiki, J. E. Her, *J. Chem, Phys.* **1994**, *101*, 9054.
[2] E. C. Muniz, G. Geuskens, *J. of Mater. Sci. – Mater. Med.* **2001**, *12*, 879.
[3] E. I. Alenichev, Z. Sedláková, M. Ilavský, *Polym. Bull.* **2007**, *58*, 191.
[4] C. Sayil, O. Okay, *Polym. Bull.* **2000**, *45*, 175.
[5] A. Naddaf, H.-J. Bart, *Proceedings of the 18th International Congress of Chemical and Process Engineering*, Prague, CHISA 2008, E7.4: 1740.
[6] B. D. Johnson, D. J. Niedermaier, W. C. Crone, J. Moorthy, D. J. Beebe, *Proceedings of the SEM Annual Conference on Experimental Mechanics*, Milwaukee, WI 2002, *129*: 1–4.
[7] N. A. Peppas, R. Langer, *Science* **1994**, *263*, 1715.
[8] D. H. Walther, G. H. Sin, H. W. Blanch, *Polym. Gels Networks.*, **1995**, *3*, 29.
[9] N. A. Peppas, P. Bures, W. Leobandung, *Eur. J. Pharm. Biopharm.* **2000**, *50*, 27.
[10] J. E. Chung, M. Yokoyama, M. Yamato, T. Aoyagi, Y. Sakurai, T. Okano, *J. Controlled Release* **1999**, *62*, 115.
[11] D. Melekaslan, N. Gundogan, O. Okay, *Polym. Bull.* **2003**, *50*, 287.
[12] J. P. Baker, L. H. Hong, H. W. Blanch, J. M. Prausnitz, *Macromo.* **1994**, *27*, 1446.
[13] S. Crump, *Composites Convention and Trade Show*, Florida 2001.
[14] O. E. Philippova, N. S. Karibyants, S. G. Stardubtzev, *Macromol.* **1994**, *27*, 2398.
[15] W. Cha, S. Hyon, D. Graiver, Y. Ikasa, *J. Appl. Polym. Sci.* **1993**, *47*, 339.
[16] K. S. Anseth, C. N. Bowman, L. Brannon-Peppas, *Biomater.* **1996**, *17*, 1647.
[17] T. Tanaka, L. O. Hocher, G. B. Benedek, *J. Chem. Phys.* **1973**, *59*(9), 5151.
[18] A. Naddaf, H.-J. Bart, I. Tsibranska, *Chem. Eng. and Process: Process Intensification* **2010**, *49*, 581.
[19] A. Naddaf, I. Tsibranska, H.-J. Bart, *Defect Diffus. Forum* **2010**, *297–301*, 664–671.
[20] A. Hüther, X. Xu, G. Maurer, *Fluid Phase Equilib.* **2006**, *240*, 186.

[21] A. Naddaf, H.-J. Bart, Defect. Diffusion, 0377-6883. Data, A. Part, *Defect Diffusion Forum*, **2011**, accepted.
[22] F. Winnik, M. Ottaviani, S. Bossman, W. Pan, M. Garcia-Garibay, N. Turro, *J. Chem. Phys.* **1993**, *97*, 12998.
[23] X. Ding, D. Fries, B. Jun, *Polym.* **2006**, *47*, 4718.
[24] Peter. J. Caspers, Gerald. W. Lucassen, Elizabeth. A. Carter, Hajo. A. Bruining, and Gerwin. J. Puppels, *J. Invest. Dermatol.* **2001**, *116*(3), 434.
[25] J. Crank, *The Mathematics of Diffusion*, Clarendon Press, Oxford 1975, p. 12.
[26] S. Kwak, M. Lafleur, *Appl Spectrosc.*, **2003**, *57*(7), 768.
[27] H. Watanabe, S. Iwata, *J. Chem. Phys.* **1996**, *105*(2), 420.
[28] K. Kosik, E. Wilk, E. Geissler, K. László, *Macromolecules*, **2007**, *40*(6), 2141.
[29] E. C. Muniz, G. Geuskens, *Macromol.* **2001**, *34*, 4480.
[30] J. W. Koros, D. R. Paul, R. Rocha, *J. Polym. Sci., Polym. Phys. Ed.* **1976**, 687.
[31] A.-C. Dubreuil, F. Doumenc, B. Guerrier, C. Allain, *Macromol.* **2003**, *36*, 5157.
[32] R. K. Lewus, G. Carta, *J. Chromatogr., A.* **1999**, *865*, 155.
[33] J. S. Vrentas, C. M. Vrentas, *J. Polym. Sci. Part B: Polym. Phys.*, **1992**, *30*(9), 1005.
[34] M. Andersson, A. Axelsson, G. Zacchi, *Int. J. Pharm.* **1997**, *157*(2), 199.
[35] M. B. Mellott, K. Searcy, M. V. Pishko, *Biomaterials* **2001**, *22*, 929.
[36] C. Khoury, T. Adalsteinsson, B. Johnson, W. C. Crone, D. J. Beebe, *Biomedical Microdevices*, **2003**, *5*(1), 35.
[37] T. Tanaka, D. Fillmore, *J. Chem. Phys.* **1979**, *70*, 1214.
[38] J. Singh, M. E. Weber, *Chem. Eng. Sci.*, **1996**, *51*(19), 4499.
[39] T. Komori, R. Sakamoto, *Colloid Polym.*, **1989**, *267*, 179.
[40] A. Peters, S. J. Candau, *Macromolecules*, **1988**, *21*(7), 2278.
[41] Y. Li, T. Tanaka, *J. Chem. Phys.*, **1990**, *92*, 1365.
[42] T. Norisuye, Q. Tran-Cong-Miyata, M. Shibayama, *Macromolecules* **2004**, *37*(8), 2944.

